doi:10.1093/brain/awt066 Brain 2013: 136; 1929–1941 | 1929

BRAIN
A JOURNAL OF NEUROLOGY

The salience network causally influences default mode network activity during moral reasoning

Winston Chiong,[1,2] Stephen M. Wilson,[1] Mark D'Esposito,[2] Andrew S. Kayser,[2,3] Scott N. Grossman,[1] Pardis Poorzand,[1] William W. Seeley,[1] Bruce L. Miller[1] and Katherine P. Rankin[1]

1 Memory and Ageing Centre, Department of Neurology, University of California, San Francisco, USA
2 Helen Wills Neuroscience Institute, University of California, Berkeley, USA
3 Ernest Gallo Clinic and Research Centre, Department of Neurology, University of California, San Francisco, USA

Correspondence to: Winston Chiong
UCSF Memory and Ageing Centre
675 Nelson Rising Lane, Suite 190
San Francisco, CA 94158, USA
E-mail: winston.chiong@ucsf.edu

Large-scale brain networks are integral to the coordination of human behaviour, and their anatomy provides insights into the clinical presentation and progression of neurodegenerative illnesses such as Alzheimer's disease, which targets the default mode network, and behavioural variant frontotemporal dementia, which targets a more anterior salience network. Although the default mode network is recruited when healthy subjects deliberate about 'personal' moral dilemmas, patients with Alzheimer's disease give normal responses to these dilemmas whereas patients with behavioural variant frontotemporal dementia give abnormal responses to these dilemmas. We hypothesized that this apparent discrepancy between activation- and patient-based studies of moral reasoning might reflect a modulatory role for the salience network in regulating default mode network activation. Using functional magnetic resonance imaging to characterize network activity of patients with behavioural variant frontotemporal dementia and healthy control subjects, we present four converging lines of evidence supporting a causal influence from the salience network to the default mode network during moral reasoning. First, as previously reported, the default mode network is recruited when healthy subjects deliberate about 'personal' moral dilemmas, but patients with behavioural variant frontotemporal dementia producing atrophy in the salience network give abnormally utilitarian responses to these dilemmas. Second, patients with behavioural variant frontotemporal dementia have reduced recruitment of the default mode network compared with healthy control subjects when deliberating about these dilemmas. Third, a Granger causality analysis of functional neuroimaging data from healthy control subjects demonstrates directed functional connectivity from nodes of the salience network to nodes of the default mode network during moral reasoning. Fourth, this Granger causal influence is diminished in patients with behavioural variant frontotemporal dementia. These findings are consistent with a broader model in which the salience network modulates the activity of other large-scale networks, and suggest a revision to a previously proposed 'dual-process' account of moral reasoning. These findings also characterize network interactions underlying abnormal moral reasoning in frontotemporal dementia, which may serve as a model for the aberrant judgement and interpersonal behaviour observed in this disease and in other disorders of social function. More broadly, these findings link recent work on the dynamic interrelationships between large-scale brain networks to observable impairments in dementia syndromes, which may shed light on how diseases that target one network also alter the function of interrelated networks.

Received November 1, 2012. Revised January 16, 2013. Accepted January 31, 2013. Advance Access publication April 9, 2013

Keywords: moral reasoning; frontotemporal dementia; salience network; default mode network; functional neuroimaging
Abbreviation: FTD = frontotemporal dementia

Introduction

The task-related functions and interrelationships of large-scale intrinsic functional brain networks are matters of controversy and ongoing investigation. A salience network anchored by the anterior insula and anterior cingulate has been hypothesized to play a central regulatory role in organizing neural responses to homeostatically significant stimuli (Dosenbach *et al.*, 2006; Seeley *et al.*, 2007; Sadaghiani *et al.*, 2010). The salience network is often activated by attention-demanding cognitive tasks, as is an executive control network including dorsal frontoparietal cortex. These networks are reciprocally related to a default mode network including the precuneus/posterior cingulate cortex, lateral parietal cortex and medial prefrontal cortex (Raichle *et al.*, 2001; Fox *et al.*, 2005). While the default mode network is deactivated by many attention-demanding tasks, it is recruited for some cognitive operations such as autobiographical memory, prospection, theory of mind, navigation, and 'personal' moral reasoning (Greene *et al.*, 2001; Harrison *et al.*, 2008; Spreng *et al.*, 2009). Consistent with a regulatory role for the salience network, recent studies provide evidence for causal influences from the salience network in modulating the activity of the default mode network and executive control network (Rilling *et al.*, 2008; Sridharan *et al.*, 2008; Bonnelle *et al.*, 2012).

These large-scale brain networks also influence the presentation and progression of neurodegenerative illnesses like Alzheimer's disease and behavioural variant frontotemporal dementia (FTD), in which the characteristic clinical courses of disease reflect the spread of pathology within targeted networks. For example, while Alzheimer's disease causes atrophy and decreased connectivity within the default mode network (Greicius *et al.*, 2004; Seeley *et al.*, 2009), behavioural variant FTD targets the salience network (Seeley *et al.*, 2009; Zhou *et al.*, 2010). Given these targeted effects, the clinical syndromes associated with these illnesses may elucidate the behavioural consequences of disruption within different networks; furthermore, understanding the interactions between large-scale networks may provide insights into the clinical progression and cognitive effects of neurodegenerative disease.

There is an apparent discrepancy, however, between results from activation-based and patient-based methods regarding the role of the default mode network in moral reasoning. In functional MRI studies of healthy subjects, nodes of the default mode network are activated during hypothetical reasoning about 'personal' moral dilemmas—e.g. dilemmas in which the best overall outcome can only be produced by violating someone's personal rights (Greene *et al.*, 2001, 2004; Harrison *et al.*, 2008). This finding might suggest that default mode network dysfunction in Alzheimer's disease should cause abnormal judgements in these dilemmas; instead, behavioural studies in patients demonstrate relatively normal personal moral judgement in Alzheimer's disease, whereas patients with behavioural variant FTD are more likely than healthy control subjects to endorse violating someone's personal rights (Mendez and Shapira, 2009). A similar pattern has been observed in patients with structural lesions to prefrontal cortex including both the medial prefrontal node of the default mode network and the anterior cingulate node of the salience network (Ciaramelli *et al.*, 2007; Koenigs *et al.*, 2007).

We aimed to reconcile the findings of activation-based and patient-based studies of the default mode network in personal moral reasoning by using functional MRI to study neural activity in patients with behavioural variant FTD and in normal control subjects during a moral reasoning task. Based on the proposed role of the salience network in regulating the activity of other brain networks, we hypothesized that the salience network plays a causal role in recruiting the default mode network during 'personal' moral dilemmas, and that abnormal moral judgement in behavioural variant FTD reflects a disruption of this causal influence. We compared univariate differences in default mode network recruitment during deliberation about personal moral dilemmas between patients with behavioural variant FTD and control subjects, and used Granger causality analysis to characterize the dynamics and directionality of network activity in patients with behavioural variant FTD and control subjects.

Materials and methods

Patients and control subjects

Eleven patients were diagnosed with behavioural variant FTD based on International Behavioral Variant FTD Criteria Consortium criteria (Rascovsky *et al.*, 2011) by a multidisciplinary team of neurologists, neuropsychologists and nurses after a comprehensive evaluation including a clinical history, neurological examination and extensive neuropsychological testing. Patients were recruited in early stages of illness because of the cognitive demands of the moral reasoning task. Of the 11 patients, one was excluded from behavioural and neuroimaging analyses for inability to perform the task (with repeated random responses prior to the complete presentation of the question prompt), and two more patients were included in behavioural analyses but excluded from neuroimaging analyses because of excessive head motion. Sixteen healthy older control subjects were verified as normal on the basis of a neurological examination, neuropsychological testing and structural MRI. Demographic, clinical and neuropsychological data for the 10 patients and 16 control subjects included in the behavioural analysis are summarized in Table 1. There was a trend towards older age in the control subjects, and a greater proportion of control subjects were female.

All participants gave written informed consent according to the Declaration of Helsinki, and the study was approved by the Committee on Human Research at UCSF.

Moral reasoning task

We modified a moral reasoning task that has been previously described (Greene *et al.*, 2001, 2004) to address criticisms of the

Table 1 Demographic, clinical and neuropsychological characteristics of patients and control subjects

Characteristics	Behavioural variant FTD ($n = 10$)	Control subjects ($n = 16$)
Demographic		
Age (years)	61.2 (6.5)	66.0 (5.5)
M/F	6/4*	6/10
Education (years)	16.6 (2.3)	17.7 (1.8)
Clinical		
MMSE (30)	28.3 (1.4)*	29.5 (0.6)
CDR total	1.1 (0.6)*	0
CDR sum of boxes	6.1 (3.4)*	0.0 (0.1)
Executive		
Digits forward	6.5 (1.4)	7.3 (1.1)
Digits backward	4.4 (1.4)*	5.5 (1.1)
Modified Trails (lines per minute)	19.2 (15.6)*	35.8 (16.2)
Stroop naming	64.1 (14.3)*	96.7 (12.1)
Stroop interference	35.8 (16.7)*	55.1 (8.3)
Calculations (5)	4.6 (0.7)	4.7 (0.5)
Language		
Boston naming test (15)	11.9 (2.5)*	14.3 (0.7)
Repetition (5)	4.3 (0.8)*	4.9 (0.3)
Auditory word recognition (PPVT, 16)	13.9 (2.3)*	15.8 (0.4)

Values represent mean (SD).
*Characteristics on which patients significantly differ from control subjects ($P < 0.05$, t-tests with unequal variance).
CDR = Clinical Dementia Severity Rating Scale; MMSE = Mini-Mental Status Examination; PPVT = Peabody Picture Vocabulary Test.

original task and to tailor the task for use in patients with dementia. These modifications are detailed in the online Supplementary material. Participants made judgements about 21 hypothetical dilemmas presented as synchronized text and audible narration through a series of three screens. The first two screens presented a vignette describing the dilemma, and the third posed a question about whether the subject would perform a hypothetical action in response to the situation ('Would you . . . in order to . . . ?'). The two vignette screens were presented over 34 s, and the question was presented over 5.5 s with an additional 6.5 s allowed for response time. Each dilemma was followed by an intertrial interval of 14 s; therefore, total presentation time for each dilemma was 1 min. Dilemmas were divided among three conditions: non-moral practical dilemmas; moral dilemmas involving an impersonal weighting of harms and benefits; and moral dilemmas involving utilitarian infringements of personal rights. Dilemmas were reviewed for content by two university professors of moral philosophy (see 'Acknowledgements' section). The text of these dilemmas is provided in Supplementary Table 1. The number of utilitarian responses and response times for each condition were compared using a general linear model procedure to delineate group differences in SAS 9.2. As a greater proportion of control subjects were female, gender was included in each of our models as an independent variable.

Participants performed the moral reasoning task while supine in the scanner; they viewed a screen through a mirror and listened to audio stimuli through padded headphones, and held a fibre-optic response pad in their right hand (with their index and middle fingers on the left and right buttons, respectively). There were three functional runs, each 420 s in duration. During each run, subjects were presented with seven dilemmas; across all three runs, the dilemmas were presented in a pseudorandomized order. Stimuli were presented and responses were recorded using E-prime (Psychology Software Tools, Inc). This was followed by T_1 structural neuroimaging; in control subjects this was followed by an 8 min resting-state functional MRI scan.

Neuroimaging acquisition

Neuroimaging data were collected on a Siemens 3 T Trio scanner. For the blood oxygen level-dependent functional MRI task paradigm, 630 T_2*-weighted echo-planar volumes were acquired with the following parameters: 29 anterior commissure-posterior commissure aligned axial slices in interleaved order; slice thickness = 3.0 mm with 15% gap; field of view 230 × 230 mm; matrix = 128 × 128; repetition time = 2000 ms; echo time = 28 ms; flip angle = 77°. For the blood oxygen level-dependent functional MRI resting-state paradigm, 240 T_2*-weighted echo-planar volumes were acquired with the following parameters: 36 anterior commissure-posterior commissure aligned axial slices in interleaved order; slice thickness = 3.0 mm with 20% gap; field of view 230 × 230 mm; matrix = 92 × 92 mm; repetition time = 2000 ms; echo time = 27 ms; flip angle = 80°.

For intersubject registration and voxel-based morphometry, a T_1-weighted 3D MP-RAGE sequence was acquired with the following parameters: 160 sagittal slices; slice thickness = 1 mm; field of view = 256 × 256 mm; matrix = 230 × 256; repetition time = 2300 ms; echo time = 2.98 ms; flip angle = 9°.

Structural neuroimaging analysis

To identify regions of atrophy, the eight subjects with behavioural variant FTD included in the neuroimaging analysis were compared with 48 normal control subjects (the 16 control subjects who took part in the functional study, plus 32 additional age- and gender-matched control subjects) with voxel-based morphometry. Structural T_1 images were initially normalized in SPM5, and more anatomically precise intersubject registration was performed with the Diffeomorphic Anatomical Registration through Exponential Lie Algebra (DARTEL) procedure (Ashburner, 2007). Subjects with behavioural variant FTD were compared with control subjects, covarying out age, gender and total intracranial volume, and all statistical maps were thresholded at voxelwise $T > 4.61$ to obtain a study-specific family-wise error threshold based upon a Monte Carlo simulation running 1000 permutations.

Functional magnetic resonance imaging univariate task activation analysis

Prior to preprocessing, all raw data were visually inspected and volumes with excessive head motion (visible interleaving artefact) or other artefacts were excluded. The number of volumes excluded was 20.0 ± 21.5 in patients with behavioural variant FTD and 3.8 ± 7.0 in control subjects. Functional MRI data were then preprocessed using standard methods in SPM5. Functional images acquired during the moral reasoning task were corrected for slice timing differences, realigned to account for within-scan head movement, unwarped to minimize susceptibility-by-movement interactions, smoothed with an 8 mm Gaussian filter, and high-pass filtered (cut-off = 128 s) to remove slow signal drift.

In our analysis, we sought to model the time period during which subjects deliberated about the moral decision. Based upon pilot testing and on observation of subjects' response times (in which subjects often responded immediately after question presentation, suggesting that they had already thought about how they would respond prior to hearing the question), we modelled this deliberation period as including the second half of the vignette presentation and the first 8 s of the question and response period [to include the mean + 1 standard deviation (SD) of the response time]. The design matrix included one explanatory variable for each of the three conditions, consisting of a boxcar function convolved with a haemodynamic response function. Several nuisance regressors were also included. The first nuisance variable, common to all three conditions, was used to model auditory, visual and language processing during the first half of the vignette. Additional covariates of no interest were included to reduce error variance: six movement parameters (three translation and three rotation parameters saved during realignment) and raw signal time courses from grey matter, white matter and CSF regions of interest. We then fit a voxel-wise general linear model to the blood oxygen level-dependent signal time course for each regressor in each participant using standard parameters [Restricted Maximum Likelihood and an autoregressive AR(1) model to correct for non-sphericity arising from serial correlations].

Random effects analyses were performed on contrast images from individual subjects, which were normalized to MNI space using the transformations derived with Unified Segmentation and DARTEL described above. Age, gender and head motion (using the root mean square of each individual's scan-to-scan translational movement in millimetres) were included as additional covariates of no interest. All contrasts were conducted across the whole brain, thresholded at voxelwise $P < 0.001$ and corrected for multiple comparisons at $P < 0.05$ based on cluster extent according to Gaussian random field theory.

Granger causality analysis

The univariate comparison between patients and control subjects (findings described below) was consistent with our hypothesis of causal influence from the salience network to the default mode network during moral reasoning. We sought further support for this hypothesis by applying Granger causality analysis, a multivariate analytic method that characterizes directional functional connections among brain regions. Granger causality analysis is based on the intuitive inference that x causes y if knowing x helps to predict the future of y. More specifically, a time series x 'Granger causes' a time series y if including past observations of x reduces the prediction error of y in a linear regression model of x and y, compared with a model that includes only past observations of y (Roebroeck *et al.*, 2005; Kayser *et al.*, 2009; Seth, 2010). The magnitude of this relationship ($F_{x\to y}$) in a bivariate analysis is expressed as the log ratio of the prediction error variances of the model including only y and of the model including x and y. This logic can be extended to a multivariate analysis, in which case the Granger causal influence from x to y, conditioned on any additional time series, is expressed as the log ratio of the prediction error variances of the model of y including every time series except x and of the model with every time series including x. It should be noted that 'Granger causal' influences (like all measures of directed functional connectivity) may not be equivalent to physical causal interactions, and may be better understood as statistical relationships characterizing the flow of information across different series of observations (Seth, 2010).

We designed our Granger causality analysis to test for causal interactions among the salience network, default mode network and executive control network; as described in the Supplementary material, we identified two primary nodes within each of these three canonical networks as regions of interest for Granger causality analysis (Sridharan *et al.*, 2008). Estimates of Granger causal influence ($F_{x\to y}$) among these six regions were computed using the Causal Connectivity Toolbox (Seth, 2010). Connections with a dominant direction of influence were identified using the difference of influence measures in either direction ($F_{x\to y} - F_{y\to x}$). We used bootstrapping techniques, block-randomizing time series to generate an empirical null distribution of Granger causal influence measures and their differences for statistical inference using functional MRI data from normal control subjects. Statistically significant Granger causal influences across subjects were identified using a Wilcoxon rank-sum test at a stringent threshold ($P < 0.01$, Bonferroni corrected). Use of the difference of influence measure for dominant directed influences allowed for a less stringent statistical threshold ($P < 0.05$, Bonferroni corrected) for these links. In a bivariate (frontoinsular→posterior cingulate cortex) analysis, Granger causal influence measures computed from normal control subjects and patients with behavioural variant FTD were compared using a Wilcoxon rank-sum test at $P < 0.05$, Bonferroni corrected.

Results

Atrophy in patients with behavioural variant frontotemporal dementia

The most markedly atrophic region in patients with behavioural variant FTD was an extensive contiguous anterior region including the bilateral striatum, orbitofrontal cortex, anterior insula, anterior temporal lobe (including amygdala), anterior cingulate cortex and frontal pole. Other foci of atrophy were found through the frontal and temporal lobes (Fig. 1 and Table 2). These regions have been characterized in previous studies as sites of atrophy in the earliest stages of behavioural variant FTD (Rosen *et al.*, 2002; Broe *et al.*, 2003; Seeley *et al.*, 2008). Many of these regions, particularly the anterior cingulate, anterior insula, orbitofrontal cortex and ventral striatum, are core nodes of the salience network.

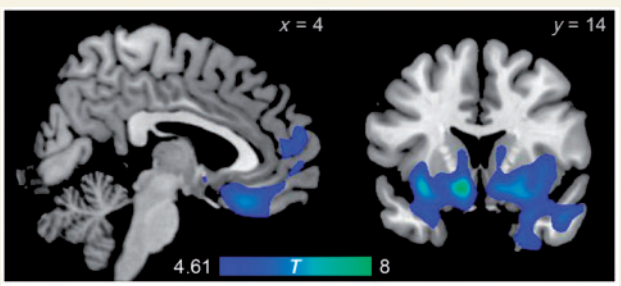

Figure 1 Regions with significantly reduced volumes in patients with behavioural variant FTD relative to normal control subjects, as revealed by voxel-based morphometry.

Table 2 Regions of significant atrophy in the behavioural variant FTD group

Region	x	y	z	Extent (mm^3)	max *T*
Bilateral ventral striatum, orbitofrontal cortex, anterior insula, anterior temporal lobe, anterior cingulate cortex, frontal pole	−10	14	−12	102 760	8.21
Right superior frontal sulcus	20	26	44	352	5.17
Right orbital sulcus	28	36	−14	320	5.19
Left orbital sulcus	−26	34	−14	128	4.88
Left middle temporal gyrus	−60	−6	−12	104	4.88
Genu of corpus callosum	−4	34	2	88	4.83
Left inferior temporal gyrus	−48	−36	−22	40	4.87
Left middle temporal gyrus	−60	8	−20	16	4.68

T statistics are thresholded based upon a Monte Carlo simulation running 1000 permutations.

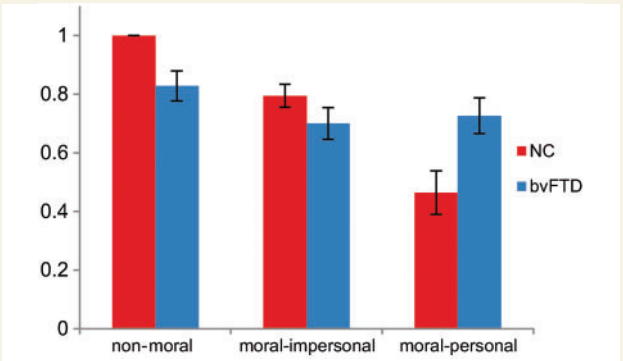

Figure 2 Proportion of utilitarian responses to non-moral, moral–impersonal, and moral–personal dilemmas in control subjects and patients. Error bars refer to the standard error of the mean. NC = normal control subjects; bvFTD = behavioural variant FTD.

Abnormally utilitarian moral reasoning in behavioural variant frontotemporal dementia

In non-moral practical dilemmas, patients with behavioural variant FTD made fewer utilitarian (in these dilemmas, personally advantageous) decisions than control subjects (83% versus 100%, $P = 0.0003$). In impersonal moral dilemmas, utilitarian decisions did not differ across groups (70% versus 80%, $P = 0.16$). In personal moral dilemmas, patients with behavioural variant FTD were more likely than control subjects to endorse utilitarian violations of personal rights (73% versus 46%, $P = 0.022$). (Fig. 2 and Supplementary material)

We observed a difference between patients and control subjects in responses to non-moral practical dilemmas, likely reflecting broader impairments in semantic processing and practical reasoning in our behavioural variant FTD cohort. To ensure that the abnormal utilitarian responses to personal moral dilemmas were not driven by these more general impairments in language and judgement, we generated an additional model incorporating subjects' responses to non-moral and moral–impersonal dilemmas as well as sex as potential confounds. In this model, the difference between patients with behavioural variant FTD and control subjects remained significant ($P = 0.041$), indicating that abnormal responses to personal moral dilemmas in behavioural variant FTD are not fully explained by generic deficits in language or practical reasoning.

Healthy older subjects recruit the default mode network during personal moral reasoning

In healthy older control subjects, no regions demonstrated significantly different patterns of activation between non-moral and moral–impersonal dilemmas. Several regions were more activated by moral–personal dilemmas than by either non-moral or moral–impersonal dilemmas, including the precuneus/posterior cingulate cortex, right angular gyrus and medial prefrontal cortex. These regions overlapped with the default mode network, as defined by a separate independent components analysis of resting-state functional MRI data from the same control subjects (Fig. 3 and Tables 3 and 4). Meanwhile, dorsal frontoparietal regions in the executive control network were less activated by moral–personal dilemmas than by either non-moral or moral–impersonal dilemmas (Fig. 4 and Tables 5 and 6). All of these findings are consistent with previous findings in young subjects (Greene *et al.*, 2001).

Default mode network recruitment during personal moral reasoning is diminished in behavioural variant frontotemporal dementia

Comparing the difference in functional activation between the moral–personal and non-moral conditions, a cluster within the bilateral posterior cingulate cortex and precuneus demonstrated a lesser increase in activity during the moral–personal condition in patients with behavioural variant FTD than in normal control subjects (Fig. 5 and Table 7). Atrophy correction was not performed on this comparison because the region of differential recruitment is distant from sites of atrophy in the behavioural variant FTD patient group. No significant between-group differences were observed when comparing the difference in functional activation between the moral–impersonal and non-moral conditions, or between the moral–personal and moral–impersonal conditions. Refer to the Supplementary material for further discussion.

The salience network exerts Granger causal influence on the default mode network during moral reasoning

Our finding that patients with behavioural variant FTD with atrophy in the salience network have reduced functional MRI recruitment in the medial parietal default mode network supports the hypothesis that the salience network causally influences the default mode network during personal moral dilemmas. More broadly, cognitive states that activate the default mode network typically deactivate the executive control network, and vice versa, and existing evidence supports a general role for the salience network in switching between these two networks in response to task demands (Rilling *et al.*, 2008; Sridharan *et al.*, 2008; Menon and Uddin, 2010; Bonnelle *et al.*, 2012). This suggests a model in which the salience network is responsible for default mode network recruitment with executive control network deactivation during personal moral dilemmas and executive control network recruitment with default mode network deactivation during non-moral and impersonal moral dilemmas. An alternative explanation is that because our behavioural variant FTD cohort also had atrophy in the medial prefrontal cortex node of the default mode network, dysfunction in this frontal node may have contributed to

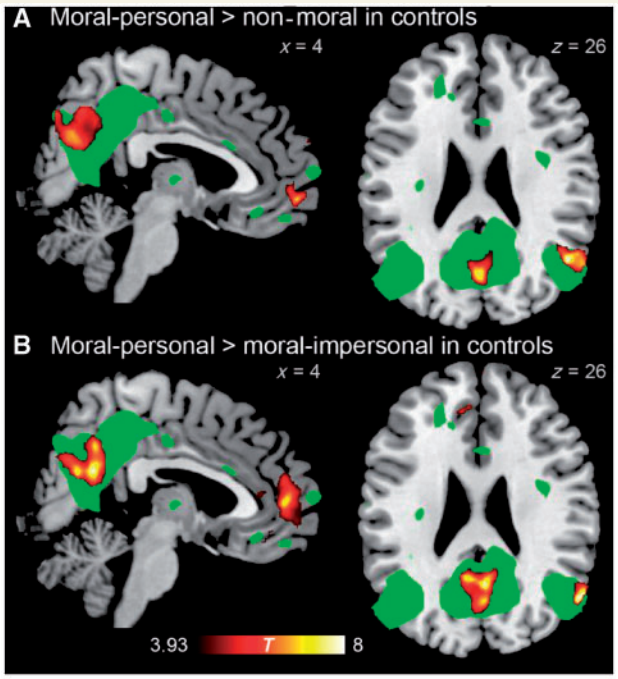

Figure 3 Brain regions demonstrating greater activity for moral–personal than for (**A**) non-moral dilemmas, and than for (**B**) moral–impersonal dilemmas in normal control subjects. For comparison, the default mode network as identified in resting state functional MRI from 15 control subjects is displayed in green at voxel-wise $P = 0.0001$.

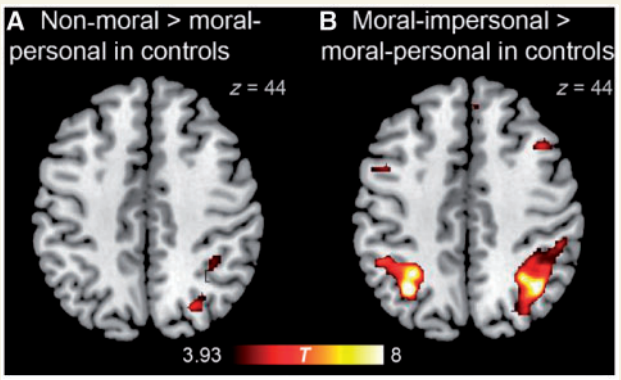

Figure 4 Brain regions demonstrating greater activity for (**A**) non-moral than for moral–personal dilemmas, and for (**B**) moral–impersonal than for moral–personal dilemmas in normal control subjects.

Table 3 Brain regions demonstrating greater activity for moral-personal than non-moral dilemmas in control subjects

Region	*x*	*y*	*z*	Extent (mm^3)	*P*	max *T*
Right angular gyrus	50	−60	26	3000	<0.001	8.46
Precuneus/posterior cingulate cortex	0	−78	42	9776	<0.001	8.30
Ventromedial prefrontal cortex, frontal pole	8	60	−4	3016	<0.001	7.99

P-values are corrected based on cluster extent, whereas max *T* is the *T* statistic of each local maximum.

Table 4 Brain regions demonstrating greater activity for moral-personal than moral-impersonal dilemmas in control subjects

Region	*x*	*y*	*z*	Extent (mm^3)	*P*	max *T*
Ventromedial prefrontal cortex, anterior cingulate cortex, frontal pole	−4	34	−14	9912	<0.001	8.28
Right angular gyrus	56	−64	26	1776	<0.001	8.27
Precuneus/posterior cingulate cortex	4	−58	24	9184	<0.001	8.21
Left putamen, globus pallidus	−20	4	−12	992	0.009	5.86

P-values are corrected based on cluster extent, whereas max *T* is the *T* statistic of each local maximum.

Table 5 Brain regions demonstrating greater activity for non-moral than moral–personal dilemmas in control subjects

Region	x	y	z	Extent (mm^3)	P	max T
Right extrastriate occipital cortex	34	−84	16	3376	<0.001	7.53
Left extrastriate occipital cortex	−22	−96	4	1512	0.002	7.08
Right middle frontal gyrus	40	−2	62	856	0.041	4.27
Right superior parietal lobule	36	−46	48	2136	<0.001	5.57
Left precentral gyrus	−34	−24	66	1192	0.009	5.49

P-values are corrected based on cluster extent, whereas max *T* is the *T* statistic of each local maximum.

Table 6 Brain regions demonstrating greater activity for moral–impersonal than moral–personal dilemmas in control subjects

Region	x	y	z	Extent (mm^3)	P	max T
Left superior parietal lobule	−32	−60	44	6776	<0.001	12.63
Right superior parietal lobule	40	−58	46	12 752	<0.001	10.28
Left middle frontal gyrus	−36	14	30	3832	<0.001	9.60
Right inferior frontal sulcus	46	38	14	3880	<0.001	9.38
Left extrastriate occipital cortex	−26	−72	30	880	0.001	8.03
Right superior frontal gyrus	8	0	52	2680	<0.001	7.97
Right middle frontal gyrus	44	20	40	2992	<0.001	7.47
Right paracingulate gyrus	4	26	48	976	0.011	7.40

P-values are corrected based on cluster extent, whereas max *T* is the *T* statistic of each local maximum.

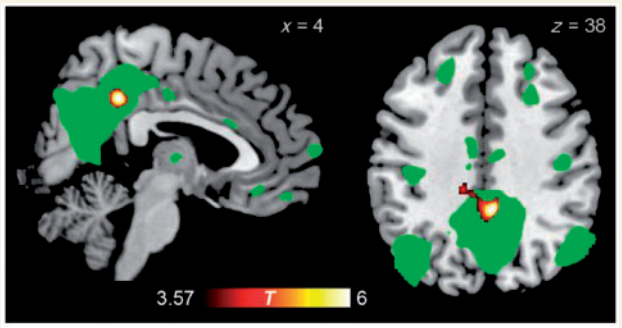

Figure 5 Brain regions demonstrating greater contrast between moral–personal and non-moral dilemmas in control subjects than in patients with behavioural variant FTD. For comparison, the default mode network as identified in resting-state functional MRI from 15 control subjects is displayed in green at voxel-wise $P = 0.0001$.

Table 7 Brain regions demonstrating greater contrast between moral–personal and non-moral dilemmas in control subjects than in patients with behavioural variant FTD

Region	x	y	z	Extent (mm^3)	P	max T
Posterior cingulate/ precuneus	4	−42	38	2112	0.003	6.84

P-values are corrected based on cluster extent, whereas max *T* is the *T* statistic of each local maximum.

abnormal recruitment of the posterior cingulate cortex node of the default mode network.

To elicit evidence for either of these hypotheses, we used Granger causality analysis to characterize directed interactions between nodes of these networks while healthy subjects performed the moral reasoning task. Using time series extracted from two primary nodes each from the salience network, default mode network and executive control network, we generated a network map representing directed functional connections between these nodes (Fig. 6 and Table 8). Granger causality analysis uncovered dominant directed influences from the salience network to the default mode network and the executive control network; including from a right frontoinsular node of the salience network to a posterior cingulate cortex node of the default mode network with reduced recruitment during personal moral reasoning in patients with behavioural variant FTD, and also from an anterior cingulate cortex node of the salience network to the medial prefrontal cortex node of the default mode network. In addition, we analysed network properties of each node during the moral reasoning task, constructing a map of Granger causal influences in each subject (links at $P < 0.01$, Bonferroni corrected) for a network analysis. This analysis demonstrated that the right frontoinsular is a causal outflow hub of the network, with the highest number of causal outflow connections (out degree) and the highest net causal outflow in control subjects (out–in degree; Supplementary Fig. 1 and Supplementary Table 2A).

Granger causal influence from the salience network to the default mode network is diminished in behavioural variant frontotemporal dementia

We then performed Granger causality analysis on time series extracted from functional MRI data from the eight patients with behavioural variant FTD in our neuroimaging analysis. We found no significant differences between the Granger causality analysis influences observed in patients with behavioural variant FTD and healthy control subjects in a multivariate analysis using six nodes to represent three canonical networks. In multivariate Granger causality analysis, the inclusion of more nodes may reduce the potential informativeness of each individual time series in predicting the other time series, which would make between-group differences in Granger influence more difficult to discern. To detect more subtle differences in Granger influence, we performed bivariate Granger causality analysis using only the frontoinsular and posterior cingulate cortex nodes. In healthy control subjects, this analysis revealed significant bidirectional Granger influences, again with a dominant direction of influence from the frontoinsular cortex to the posterior cingulate cortex. In this bivariate analysis, the Granger influence from the frontoinsular cortex to the posterior cingulate cortex was reduced in patients with behavioural variant FTD compared with control subjects (median 0.0161 versus 0.0448, $P = 0.016$). Refer to the Supplementary material for further discussion. Finally, in an analysis of network properties the right frontoinsular cortex was also the only node with significantly disrupted inflow and outflow network properties in patients with behavioural variant FTD (Supplementary Table 2B; out degree $P = 0.043$, in degree $P = 0.022$; one-tailed t-test not corrected for multiple comparisons).

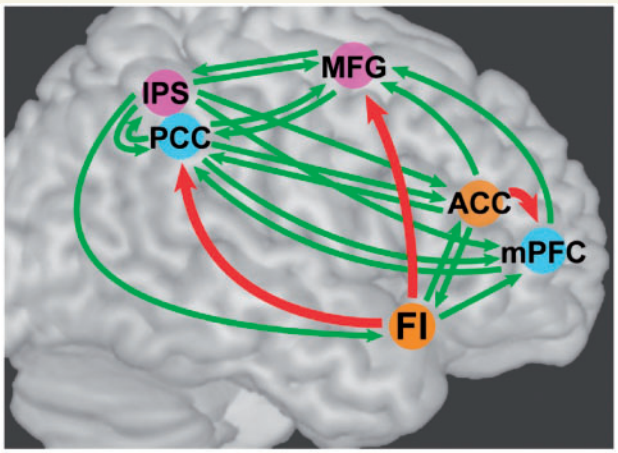

Figure 6 Granger causality analysis of key nodes of the salience (orange), default mode (blue), and executive control (pink) networks during the moral reasoning task. Connections with significant Granger influences at the group level (Wilcoxon rank-sum test, $P < 0.01$, Bonferroni corrected) are depicted in green; a subset of these connections with a dominant direction of influence (Wilcoxon rank-sum test, $P < 0.05$, Bonferroni corrected) are depicted in red. ACC = anterior cingulate cortex; FI = frontoinsular; IPS = intraparietal sulcus; MFG = middle frontal gyrus; mPFC = medial prefrontal cortex; PCC = posterior cingulate cortex.

Individual relationships among neuroimaging and behavioural measures

In addition to group-level differences between patients with behavioural variant FTD and normal control subjects, we also explored relationships between measures of behaviour, univariate functional MRI activation and Granger causal influence across individual subjects. As noted above, patients with behavioural variant FTD had diminished Granger causal influence in a bivariate analysis from the frontoinsular cortex to the posterior cingulate cortex, and also had reduced recruitment of the posterior cingulate cortex during personal moral reasoning. Although we did not observe a significant correlation between Granger influence and

Table 8 Granger causal influences across nodes (column→row)

$F_{col->row}$	FI	ACC	mPFC	PCC	MFG	IPS
FI	–	0.0500 ± 0.0136	0.0206 ± 0.0067	0.0141 ± 0.0045	0.0144 ± 0.0042	0.0167 ± 0.0053
ACC	0.0459 ± 0.0149	–	0.0092 ± 0.0022	0.0180 ± 0.0040	0.0249 ± 0.0079	0.0177 ± 0.0040
mPFC	0.0214 ± 0.0047	0.0298 ± 0.0087 ($P = 0.0001$)	–	0.0211 ± 0.0055	0.0083 ± 0.0022	0.0119 ± 0.0027
PCC	0.0309 ± 0.0072 ($P = 0.0007$)	0.0109 ± 0.0023	0.0118 ± 0.0038	–	0.0183 ± 0.0064	0.0252 ± 0.0104
MFG	0.0277 ± 0.0065 ($P = 0.0019$)	0.0163 ± 0.0039	0.0128 ± 0.0033	0.0177 ± 0.0040	–	0.0268 ± 0.0053
IPS	0.0252 ± 0.0069	0.0098 ± 0.0025	0.0132 ± 0.0045	0.0357 ± 0.0122	0.0281±0.0063	–

Cells coloured in green represent directed functional connections that significantly differ from the null distribution at a stringent threshold of $P < 0.01$ corrected for 30 comparisons. Cells outlined in red represent dominant directed influences that significantly differ from the null distribution at a threshold of $P < 0.05$ corrected for 15 comparisons.

FI = frontoinsular; ACC = anterior cingulate cortex; mPFC = medial prefrontal cortex; PCC = posterior cingulate cortex; MFG = middle frontal gyrus; IPS = intraparietal sulcus.

recruitment of the posterior cingulate cortex during personal moral reasoning (i.e. the difference in activation between the moral–personal and non-moral condition), we did observe a correlation between Granger influence and the beta estimate of posterior cingulate cortex activation during personal moral reasoning alone (Spearman's rho = 0.47, $P = 0.022$; Supplementary Fig. 2).

We found weaker evidence for correlations between individual behaviour and individual neuroimaging measures. As predicted by group findings across patients and normal control subjects, there was a negative correlation between the proportion of utilitarian choices and the beta estimate of posterior cingulate cortex activation during personal moral reasoning (Pearson's $r = -0.37$, one-tailed $P = 0.036$). There was also a trend towards a negative correlation between the proportion of utilitarian choices and Granger influence (in a bivariate analysis) from the frontoinsular cortex to the posterior cingulate cortex. Using a median split to dichotomize participants into more and less utilitarian moral reasoners, the less utilitarian reasoners had greater measures of Granger influence (median 0.0490 versus 0.0181, one-tailed $P = 0.032$).

Discussion

We present here four converging lines of evidence incorporating behavioural, univariate functional neuroimaging, and multivariate functional neuroimaging methods, in both patients and healthy control subjects, which together support a causal influence from the salience network to the default mode network during moral reasoning. First (as previously reported), healthy subjects recruit the default mode network when deliberating about personal moral dilemmas, yet patients with behavioural variant FTD, whose disease preferentially targets the salience network, give abnormally utilitarian responses to these dilemmas. Second, patients with behavioural variant FTD have reduced recruitment of the default mode network compared with normal control subjects when deliberating about these dilemmas. Third, Granger causality analysis of functional MRI data from normal control subjects indicates that nodes of the salience network exert directed influence on nodes of the default mode network during performance of a moral reasoning task. Fourth, this directed functional connectivity from the salience network to the default mode network is diminished in patients with behavioural variant FTD. This causal hypothesis resolves an apparent discrepancy between patient-based and activation-based studies of moral reasoning, and coheres with other studies that support a causal role for the salience network in modulating default mode network activity in response to task demands. One recent study used chronometric and Granger causality analysis techniques to indicate that the salience network (especially the right frontoinsular cortex) plays a critical role in switching between default mode network and executive control network during both task-related and resting states (Sridharan *et al*., 2008). Another Granger causality analysis analysis using a socially interactive task indicated that the bilateral frontoinsular and anterior cingulate cortex causally influence the medial prefrontal node of the default mode network, with greater influence during a social condition than during a non-social control condition (Rilling *et al*., 2008). And in a study of patients with traumatic brain injury, aberrant default mode network deactivation during an attention-demanding task was specifically predicted by loss of fractional anisotropy in the white matter tract between the right frontoinsular cortex and anterior cingulate cortex (Bonnelle *et al*., 2012).

The present study extends these earlier findings by combining patient-based methods with measures of functional connectivity, and by linking disruption of this causal relationship to salience network-related social and behavioural abnormalities that are characteristic of behavioural variant FTD (Zhou *et al*., 2010). Discovering causal relationships between large-scale networks in the setting of neurodegenerative diseases that target particular networks is likely to be crucial in advancing our understanding of how these and other diseases produce cognitive effects in distant, interconnected brain regions. Unfortunately, inferential support for such causal hypotheses using patient studies or activation data is almost always indirect, relying upon methodological and neuroscientific assumptions that are open to question. We believe that the convergence of findings from different methods is a strength of this study, as different findings rely upon different assumptions.

To make these assumptions explicit, one finding in support of our hypothesis is that patients with behavioural variant FTD with atrophy in the salience network have reduced recruitment of the posterior cingulate cortex node of the default mode network during personal moral reasoning as compared with healthy control subjects. An interpretive difficulty often encountered in univariate comparisons of functional MRI activity between patients and control subjects is that activation differences may be confounded by haemodynamic, metabolic or other uncontrolled local physiological differences between groups, aside from the neural difference of interest (D'Esposito *et al*., 2003). This concern is mitigated in the present study by the fact that the posterior cingulate cortex is distant from sites of regional atrophy in our patient cohort (Fig. 1). However, there may also have been true neural differences in recruitment (for instance, in the medial prefrontal node of the default mode network, which was also atrophied in our patient cohort) that we were unable to detect due to these physiological confounds.

Another finding in support of our hypothesis is the network map (Fig. 6) generated by our Granger causality analysis of functional MRI data from healthy older control subjects during the moral reasoning task. This finding does not involve patient data or on group differences, and so does not rely on the same assumptions as the univariate finding. Granger causality analysis and a related analytical technique, dynamic causal modelling, are two broadly used methods for discovering directed influences using functional MRI data (Valdes-Sosa *et al*., 2011); dynamic causal modelling was not appropriate to our task because the temporal properties of each vignette relevant to moral reasoning could not be precisely specified in advance. The methodological literature on Granger causality analysis has focused on two potential difficulties: regional differences in haemodynamic lag and downsampling. To illustrate the first problem, functional MRI blood oxygen level-dependent signal measures blood oxygenation rather than neural activity directly, so in theory if the haemodynamic response to neural activity in region x is faster than in region y, the blood oxygen level-dependent time course in region x could 'predict' the blood

oxygen level-dependent time course in region *y* even if neural events in both regions are concurrent (or even if neural events in *y* precede those in *x* but by less than the difference in haemodynamic lag). Several studies using simulations and actual functional MRI data have been performed to evaluate this possibility, with some indicating that Granger influences in functional MRI studies are therefore vulnerable to spurious findings (David *et al.*, 2008; Smith *et al.*, 2011), and others indicating that the method is robust enough that significant Granger influences are unlikely to be attributable solely to such confounds (Deshpande *et al.*, 2010; Schippers *et al.*, 2011; Seth *et al.*, 2013). To illustrate the second problem, whereas neural events occur on a millisecond timescale, data acquisition in functional MRI typically occurs on a second timescale (the repetition time in our study was 2 s). The information lost in downsampling increases the prediction error of *y* in a linear regression model including past observations of *y*; but if *x* and *y* are correlated (even if because *y* causally influences *x*), then some of *y*'s lost information can be reintroduced by including *x* in the model, reducing the prediction error of *y* without reflecting a true directed influence from *x* to *y* (Roebroeck *et al.*, 2005; Seth *et al.*, 2013). For our main Granger causality analysis finding we used the difference of influence measures in either direction ($F_{x\rightarrow y} - F_{y\rightarrow x}$), which is standardly applied to avoid spurious directionality due to downsampling (Roebroeck *et al.*, 2005). Still, given these ongoing methodological controversies, we regard this Granger causality analysis as offering additional evidence in favour of our hypothesis, rather than as decisive on its own.

Finally, we found that Granger causal influence from the frontoinsular to the posterior cingulate cortex during moral reasoning was diminished in patients with behavioural variant FTD. This finding may unify the findings of our univariate comparison between patients and control subjects with the findings of our Granger causality analysis in control subjects, although the interpretation of this finding does depend on many of the same assumptions as these other two findings. In particular, the frontoinsular node used in our Granger causality analysis is based on a local statistical peak of atrophy in the behavioural variant FTD cohort (as detailed in the Supplementary material). It is possible that the reduced Granger causal influence and disrupted network properties of this node in patients (Supplementary Table 2B) reflect reduced fidelity of the functional MRI blood oxygen level-dependent signal due to atrophy or other regional physiological confounds, rather than alterations of neural activity itself. This concern applies not only to the present finding, but also to many other functional MRI studies of functional connectivity or network properties in brain regions affected by disease. We note also that neuronal loss and local physiological derangements likely are not independent from neural dysfunction, but instead are likely to be related and in some respects, causative. Here again, we believe that the most important observation is that this finding supports the same causal hypothesis as our other findings.

A revised two-process model of moral judgement

Earlier functional MRI studies of personal moral reasoning were initially thought to support a dual process model of moral judgement, in which a cognitive/rational system subserves utilitarian moral reasoning and an emotional system subserves counter-utilitarian moral reasoning (Greene *et al.*, 2001, 2004). This interpretation was based on the claim that the precuneus/posterior cingulate cortex, lateral parietal cortex and medial prefrontal cortex, which are recruited during personal moral judgement, are specifically involved in emotion processing. However, subsequent research indicates that what unifies these regions is not a shared relationship to emotional processing (though the medial prefrontal cortex does subserve emotional processes that likely are relevant to moral reasoning), but instead that they are nodes of the default mode network (Harrison *et al.*, 2008). Furthermore, more detailed analysis of reaction time data used to support the model does not support the proposed interpretation (McGuire *et al.*, 2009).

Although current evidence does not support the claim that personal moral judgement involves a conflict between specifically emotional and rational processes, it remains notable that the default mode network is more activated by moral–personal than by non-moral or moral–impersonal dilemmas, while the executive control network is more activated by non-moral and moral–impersonal than moral–personal dilemmas. The differential engagement of these two networks does suggest that two distinct cognitive processes may be engaged by moral reasoning, and that they respond differently based on the content of the moral problem under consideration.

Given previous research that implicates the salience network in attention, alertness and in switching between the default mode network and executive control network (Dosenbach *et al.*, 2006; Seeley *et al.*, 2007; Sridharan *et al.*, 2008; Menon and Uddin, 2010; Nelson *et al.*, 2010), we suggest that the salience network plays an alerting and switching role during moral reasoning. In personal moral dilemmas, the salience network utilizes social and emotional resources to identify the personal nature of these dilemmas and then recruits the default mode network; whereas in other decisions, the salience network recruits the executive control network. This model predicts that in behavioural variant FTD, salience network dysfunction will result in failure to recognize the personal nature of these dilemmas, which in turn leads to a failure to appropriately recruit the non-targeted default mode network. The behavioural manifestation of these abnormal relationships between networks would be a tendency to deliberate about personal moral dilemmas in a manner analogous to the way healthy control subjects deliberate about non-moral and impersonal moral dilemmas, where personal rights are not at stake.

If the default mode network as a network does not specifically subserve emotional processing, the question remains why it is recruited in moral dilemmas with personal content. We note that one feature that unifies many of the cognitive operations that engage the default mode network—such as retrieving autobiographical memories, envisioning the future, navigating spatial environments, and inferring other people's states of mind—is that they involve the construction of dynamic mental simulations of states of affairs that are not presently available in sense experience (Tulving, 1983; Suddendorf and Corballis, 1997; Buckner *et al.*, 2008; Spreng and Grady, 2010). One link with moral reasoning may be that in personal, more than impersonal moral dilemmas, the deliberator must often simulate the subjective

points of view of the agent or of other affected parties. For example, in the case of an impersonal moral dilemma, if a policy would be better for many people and worse (to an equivalent degree) for a few, it would be natural to decide in favour of this policy on the basis of expected utility, without engaging in a mental simulation of any affected person's point of view. However, when deliberating about whether to push an innocent person into the path of a trolley that would otherwise kill five, it is natural to imagine 'what it would be like' to push the innocent person, or to be the person pushed, or to be one of the five that would be saved.

The default mode network's role in mental simulation may provide a neuroscientific framework for the philosophical claim that counter-utilitarian moral reasoning is closely tied to a personal point of view, while utilitarian moral reasoning is tied to an objective conception of the world without reference to any individual perspective. For instance, Rawls (1971) argued that utilitarianism does not properly account for the distinctness of persons; Nagel (1986) proposed an account of personal rights that appeals to the perspective of the moral agent, and Kamm (1992) has developed an alternative that appeals to the perspective of the person whose rights are violated. If deliberation about personal rights requires one to adopt a personal point of view, one role of the default mode network in personal moral reasoning may be to access different relevant points of view (both of the agent and of those affected by the action) by mental simulation. Conversely, the executive control network would be engaged by judgements that do not require such a simulation, such as those non-moral and impersonal moral dilemmas that can be resolved by a calculation of expected utilities.

In summary, our findings reconcile a discrepancy between previous activation-based and patient-based studies of the role of the default mode network in moral reasoning, and suggest a revision to an influential dual-process account of moral reasoning. While our model has been developed using findings from behavioural variant FTD, the model has implications for other socio-emotional disorders associated with abnormalities in personal moral judgement such as psychopathy (Pujol *et al.*, 2011), medial prefrontal structural brain lesions (Ciaramelli *et al.*, 2007; Koenigs *et al.*, 2007), alcoholism (Khemiri *et al.*, 2012), and autism (Gleichgerrcht *et al.*, 2012), particularly as evidence accumulates that all of these disorders may involve disruption of the salience network (Bjork *et al.*, 2008; Di Martino *et al.*, 2009; Nomura *et al.*, 2010; Ly *et al.*, 2012; von dem Hagen *et al.*, 2012). In all of these disorders, a central question concerns the functional interrelationship between networks that are targeted by disease and networks that are relatively spared. Our findings contribute to existing research indicating a central role for the salience network in modulating and regulating the activity of other large-scale networks such as the default mode network, which may help to explain the profound behavioural consequences of injury to the salience network in behavioural variant FTD and other disorders.

Limitations

Our study was limited in the number of subjects with behavioural variant FTD available for study (as the extensive cognitive demands of the task limited recruitment to patients in the earliest stages of disease) and also in the number of trials available for each subject (given reduced patient tolerance for testing and the long trials required by our vignette-based paradigm). This precluded potentially informative analyses, such as comparisons between activation preceding utilitarian and non-utilitarian responses within each condition, or comparisons between utilitarian responses to moral–personal dilemmas in patients and control subjects.

Given difficulties inherent to functional MRI in patient populations, and in matching disease cohorts to healthy cohorts, we chose to focus this study on moral reasoning in behavioural variant FTD and did not include an Alzheimer's disease comparison group. It remains unclear why patients with Alzheimer's disease and atrophy in the default mode network give normal responses to these dilemmas; one potential explanation is that the medial prefrontal cortex node is less affected than more posterior nodes of the default mode network in Alzheimer's disease. This node may serve as a transition zone between the default mode network and salience network given its functional connectivity with orbitofrontal and ventral striatal regions involved in salience processing (Greicius *et al.*, 2003) and its involvement in socio-emotional reasoning (Amodio and Frith, 2006). Future studies of activation and network dynamics during moral reasoning in early Alzheimer's disease may be useful in evaluating this hypothesis, and may help to clarify the cognitive contributions and interrelationships of different subsystems within the default mode network (Andrews-Hanna *et al.*, 2010).

Acknowledgements

We thank Helen (Juan) Zhou and Devarajan Sridharan for methodological assistance and discussion; Agnieszka Jaworska and Ryan Preston for philosophical review of the content of vignettes; Matthew Growdon and Jung Jang for administrative support; and our healthy volunteers, patients, and patients' families for their generous participation in research.

Funding

This work was supported by the UCSF Flexible Neurology Residency and the American Brain Foundation/Alzheimer's Association Robert Katzman, MD Clinical Research Training Fellowship to W.C.; the Larry Hillblom Foundation to B.L.M.; and the National Institutes of Health [R01-AG029577-01 to K.P.R., P01-AG019724 to B.L.M., and NS40813 and MH 63901 to M.D.].

Supplementary material

Supplementary material is available at *Brain* online.

References

Amodio DM, Frith CD. Meeting of minds: the medial frontal cortex and social cognition. Nat Rev Neurosci 2006; 7: 268–77.

Andrews-Hanna JR, Reidler JS, Sepulcre J, Poulin R, Buckner RL. Functional-anatomic fractionation of the brain's default network. Neuron 2010; 65: 550–62.

Ashburner J. A fast diffeomorphic image registration algorithm. Neuroimage 2007; 38: 95–113.
Barnett L, Seth AK. Behaviour of Granger causality under filtering: theoretical invariance and practical application. J Neurosci Methods 2011; 201: 404–19.
Bjork JM, Smith AR, Hommer DW. Striatal sensitivity to reward deliveries and omissions in substance dependent patients. Neuroimage 2008; 42: 1609–21.
Bonnelle V, Ham T, Leech R, Kinnunen KM, Mehta MA, Greenwood RJ, et al. Salience network integrity predicts default mode network function after traumatic brain injury. Proc Natl Acad Sci USA 2012; 109: 4690–5.
Broe M, Hodges J, Schofield E, Shepherd C, Kril J, Halliday G. Staging disease severity in pathologically confirmed cases of frontotemporal dementia. Neurology 2003; 60: 1005–11.
Buckner RL, Andrews-Hanna JR, Schacter DL. The brain's default network: anatomy, function, and relevance to disease. Ann N Y Acad Sci 2008; 1124: 1–38.
Ciaramelli E, Muccioli M, Làdavas E, di Pellegrino G. Selective deficit in personal moral judgment following damage to ventromedial prefrontal cortex. Soc Cogn Affect Neurosci 2007; 2: 84–92.
D'Esposito M, Deouell LY, Gazzaley A. Alterations in the BOLD fMRI signal with ageing and disease: a challenge for neuroimaging. Nat Rev Neurosci 2003; 4: 863–72.
David O, Guillemain I, Saillet S, Reyt S, Deransart C, Segebarth C, et al. Identifying neural drivers with functional MRI: an electrophysiological validation. PLoS Biol 2008; 6: 2683–97.
Deshpande G, Sathian K, Hu X. Effect of hemodynamic variability on Granger causality analysis of fMRI. Neuroimage 2010; 52: 884–96.
Di Martino A, Ross K, Uddin LQ, Sklar AB, Castellanos FX, Milham MP. Functional brain correlates of social and nonsocial processes in autism spectrum disorders: an activation likelihood estimation meta-analysis. Biol Psychiatry 2009; 65: 63–74.
Dosenbach NU, Visscher KM, Palmer ED, Miezin FM, Wenger KK, Kang HC, et al. A core system for the implementation of task sets. Neuron 2006; 50: 799–812.
Fox MD, Snyder AZ, Vincent JL, Corbetta M, Van Essen DC, Raichle ME. The human brain is intrinsically organized into dynamic, anticorrelated functional networks. Proc Natl Acad Sci USA 2005; 102: 9673–8.
Gleichgerrcht E, Torralva T, Rattazzi A, Marenco V, Roca M, Manes F. Selective impairment of cognitive empathy for moral judgment in adults with high functioning autism. Soc Cogn Affect Neurosci 2012. [Epub ahead of print].
Greene JD, Nystrom LE, Engell AD, Darley JM, Cohen JD. The neural bases of cognitive conflict and control in moral judgment. Neuron 2004; 44: 389–400.
Greene JD, Sommerville RB, Nystrom LE, Darley JM, Cohen JD. An fMRI investigation of emotional engagement in moral judgment. Science 2001; 293: 2105–8.
Greicius MD, Krasnow B, Reiss AL, Menon V. Functional connectivity in the resting brain: a network analysis of the default mode hypothesis. Proc Natl Acad Sci USA 2003; 100: 253–8.
Greicius MD, Srivastava G, Reiss AL, Menon V. Default-mode network activity distinguishes Alzheimer's disease from healthy aging: evidence from functional MRI. Proc Natl Acad Sci USA 2004; 101: 4637–42.
Harrison BJ, Pujol J, López-Solà M, Hernández-Ribas R, Deus J, Ortiz H, et al. Consistency and functional specialization in the default mode brain network. Proc Natl Acad Sci USA 2008; 105: 9781–6.
Kamm FM. Non-consequentialism, the person as an end-in-itself, and the significance of status. Philos Public Aff 1992; 21: 354–89.
Kayser AS, Sun FT, D'Esposito M. A comparison of Granger causality and coherency in fMRI-based analysis of the motor system. Hum Brain Mapp 2009; 30: 3475–94.
Khemiri L, Guterstam J, Franck J, Jayaram-Lindström N. Alcohol dependence associated with increased utilitarian moral judgment: a case control study. PLoS One 2012; 7: e39882.
Koenigs M, Young L, Adolphs R, Tranel D, Cushman F, Hauser M, et al. Damage to the prefrontal cortex increases utilitarian moral judgements. Nature 2007; 446: 908–11.
Ly M, Motzkin J, Philippi C, Kirk GR, Newman JP, Kiehl KA, et al. Cortical thinning in psychopathy. Am J Psychiatry 2012; 169: 743–9.
McGuire J, Langdon R, Coltheart M, Mackenzie C. A reanalysis of the personal/impersonal distinction in moral psychology research. J Exp Soc Psychol 2009; 45: 577–80.
Mendez MF, Shapira JS. Altered emotional morality in frontotemporal dementia. Cogn Neuropsychiatry 2009; 14: 165–79.
Menon V, Uddin LQ. Saliency, switching, attention and control: a network model of insula function. Brain Struct Funct 2010; 214: 655–67.
Nagel T. The view from nowhwere. Oxford: Oxford University Press; 1986.
Nelson SM, Dosenbach NU, Cohen AL, Wheeler ME, Schlaggar BL, Petersen SE. Role of the anterior insula in task-level control and focal attention. Brain Struct Funct 2010; 214: 669–80.
Nomura EM, Gratton C, Visser RM, Kayser A, Perez F, D'Esposito M. Double dissociation of two cognitive control networks in patients with focal brain lesions. Proc Natl Acad Sci USA 2010; 107: 12017–22.
Pujol J, Batalla I, Contreras-Rodríguez O, Harrison BJ, Pera V, Hernández-Ribas R, et al. Breakdown in the brain network subserving moral judgment in criminal psychopathy. Soc Cogn Affect Neurosci 2011; 7: 917–23.
Raichle ME, MacLeod AM, Snyder AZ, Powers WJ, Gusnard DA, Shulman GL. A default mode of brain function. Proc Natl Acad Sci USA 2001; 98: 676–82.
Rascovsky K, Hodges J, Knopman D, Mendez MF, Kramer JH, Neuhaus J, et al. Sensitivity of revised diagnostic criteria for the behavioural variant of frontotemporal dementia. Brain 2011; 134: 2456–77.
Rawls J. A theory of justice. Cambridge, MA: Harvard University Press; 1971.
Rilling JK, Dagenais JE, Goldsmith DR, Glenn AL, Pagnoni G. Social cognitive neural networks during in-group and out-group interactions. Neuroimage 2008; 41: 1447–61.
Roebroeck A, Formisano E, Goebel R. Mapping directed influence over the brain using Granger causality and fMRI. Neuroimage 2005; 25: 230–42.
Rosen HJ, Gorno-Tempini ML, Goldman WP, Perry RJ, Schuff N, Weiner M, et al. Patterns of brain atrophy in frontotemporal dementia and semantic dementia. Neurology 2002; 58: 198–208.
Sadaghiani S, Scheeringa R, Lehongre K, Morillon B, Giraud AL, Kleinschmidt A. Intrinsic connectivity networks, alpha oscillations, and tonic alertness: a simultaneous electroencephalography/functional magnetic resonance imaging study. J Neurosci 2010; 30: 10243–50.
Schippers MB, Renken R, Keysers C. The effect of intra- and inter-subject variability of hemodynamic responses on group level Granger causality analyses. Neuroimage 2011; 57: 22–36.
Seeley WW, Crawford R, Rascovsky K, Kramer JH, Weiner M, Miller BL, et al. Frontal paralimbic network atrophy in very mild behavioral variant frontotemporal dementia. Arch Neurol 2008; 65: 249–55.
Seeley WW, Crawford RK, Zhou J, Miller BL, Greicius MD. Neurodegenerative diseases target large-scale human brain networks. Neuron 2009; 62: 42–52.
Seeley WW, Menon V, Schatzberg AF, Keller J, Glover GH, Kenna H, et al. Dissociable intrinsic connectivity networks for salience processing and executive control. J Neurosci 2007; 27: 2349–56.
Seth AK. A MATLAB toolbox for Granger causal connectivity analysis. J Neurosci Methods 2010; 186: 262–73.
Seth AK, Chorley P, Barnett LC. Granger causality analysis of fMRI BOLD signals is invariant to hemodynamic convolution but not downsampling. NeuroImage 2013; 65: 540–55.
Smith SM, Miller KL, Salimi-Khorshidi G, Webster M, Beckmann CF, Nichols TE, et al. Network modelling methods for fMRI. NeuroImage 2011; 54: 875–91.
Spreng RN, Grady CL. Patterns of brain activity supporting autobiographical memory, prospection, and theory of mind, and their

relationship to the default mode network. J Cogn Neurosci 2010; 22: 1112–23.
Spreng RN, Mar RA, Kim AS. The common neural basis of autobiographical memory, prospection, navigation, theory of mind, and the default mode: a quantitative meta-analysis. J Cogn Neurosci 2009; 21: 489–510.
Sridharan D, Levitin DJ, Menon V. A critical role for the right fronto-insular cortex in switching between central-executive and default-mode networks. Proc Natl Acad Sci USA 2008; 105: 12569–74.
Suddendorf T, Corballis MC. Mental time travel and the evolution of the human mind. Genet Soc Gen Psychol Monogr 1997; 123: 133–67.
Tulving E. Elements of episodic memory. Oxford: Clarendon Press; 1983.
Valdes-Sosa PA, Roebroeck A, Daunizeau J, Friston K. Effective connectivity: Influence, causality and biophysical modeling. Neuroimage 2011; 58: 339–61.
von dem Hagen EA, Stoyanova RS, Baron-Cohen S, Calder AJ. Reduced functional connectivity within and between 'social' resting state networks in autism spectrum conditions. Soc Cogn Affect Neurosci 2012. [Epub ahead of print].
Zhou J, Greicius MD, Gennatas ED, Growdon ME, Jang JY, Rabinovici GD, et al. Divergent network connectivity changes in behavioural variant frontotemporal dementia and Alzheimer's disease. Brain 2010; 133: 1352–67.